ACS Macro Letters

pubs.acs.org/macroletters Letter

Glycine *N*-Thiocarboxyanhydride: A Key to Glycine-Rich Protein Mimics

Jianping Wang, Peng Zhou, Ting Shen, Songyi Xu, Tianwen Bai, and Jun Ling*

Cite This: *ACS Macro Lett.* 2023, 12, 1466−1471 Read Online

ACCESS | Metrics & More | Article Recommendations | Supporting Information

ABSTRACT: Glycine-rich proteins (GRPs) containing a high content of glycine residues (>30%) possess unique structural stability. However, the controllable synthesis of glycine-rich poly(amino acid)s (PAAs) to mimic GRPs has not been realized yet due to the poor solubility of polyglycine segments. We developed a novel method to synthesize glycine-rich PAAs via the controlled ring-opening copolymerization of glycine-*N*-thiocarboxyanhydrides (Gly-NTA) with sarcosine-*N*-carboxyanhydride and *ε*-Cbz-L-lysine-*N*-carboxyanhydride. The random copolymerization is evidenced by a kinetic study that shows that the propagation rate constant of Gly-NTA is close to those of comonomers. The copolymers exhibit predictable molecular weights between 4.5 and 24.6 kg/mol and tunable glycine incorporation, varying from 10.3 to 59.2%. Poly(Gly-*r*-Sar) samples with various glycine contents form nanoparticles or a hydrogel in water. Remarkably, the *β*-sheet folding of poly(Gly-*r*-Lys) remains intact in a neutral environment where the amine groups are protonated. Overall, the strategy paves the way to engineer glycine-rich PAAs and thereby expands their applications.

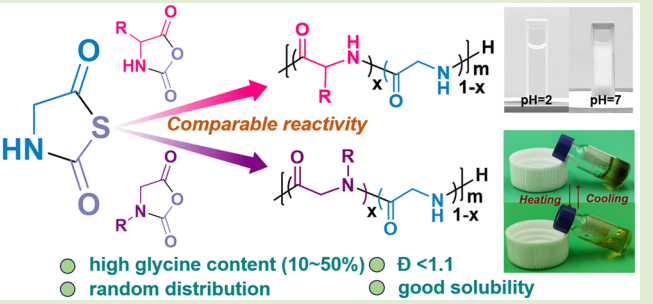

Proteins are natural biomacromolecules composed of *α*-amino acids. Tremendous hydrogen-bond donors and acceptors enable proteins to maintain highly organized structures for vital activities. In particular, glycine-rich proteins (GRPs) possess multiple functions including providing mechanical strength to cell walls and acting as velcro in the protein−protein interaction.[1−3] The key to the significant strength of GRPs is abundant *β*-sheet structures in glycine-rich regions that do not contain long polyglycine (PGly) segments, but do contain repeating sequences such as GGGX and GGXXXGG, where G is glycine and X is any other amino acid residue.[3−5] In other words, peptides that constitute GRPs are regarded as random poly(amino acid)s (PAAs) rather than block ones. Mimicking GRPs and their functions is an appealing, yet challenging issue. Solid phase peptide synthesis (SPPS) has been employed to produce glycine-rich PAAs, which is unfavorable in industry due to its tedious procedure and limited molecular weights (MWs).[6−8] Ring-opening polymerization (ROP) of amino acid *N*-carboxyanhydrides (NCAs) is a promising method to synthesize random high-MW PAAs.[9−11] However, the controlled polymerization of glycine NCA (Gly-NCA) has not yet been realized yet. Short PGly segments with more than five residues can arrange to ordered antiparallel *β*-sheet structures, which reduces the solubility of the product dramatically and prevents further polymerization.[12−14]

Inserting a second monomer to weaken the *β*-sheet is a feasible solution.[15,16] Wooley et al. utilized PEG_{45}-NH_2 to initiate the copolymerization of Gly-NCA with *γ*-benzyl-L-glutamate-NCA (BLG-NCA). However, Gly-NCA was consumed much faster than sterically hindered BLG-NCA. Homopolymeric PGly blocks were generated, which led to gelation during polymerization and poor solubility in organic solvents.[17] Thus, Gly-NCA is not suitable for the controlled synthesis of glycine-rich PAAs. *N*-Thiocarboxyanhydrides (NTAs), thio-analogues of NCAs, are more stable monomers with decreased reactivity.[18,19] In this contribution, we realized the controlled random copolymerization of Gly-NTA with *α*-amino acid NCAs. *β*-Sheet folding of glycine residues in products is suppressed to form any gel or turbidness during polymerization, while the obtained glycine-rich PAAs exhibit excellent thermo- and pH-responsive properties to realize sol−gel transition and pH-dependent aggregation based on the formation of secondary structures.

Gly-NTA is prepared via the cyclization of *N*-ethoxythiocarbonyl glycine in the presence of PBr_3 (see the experimental section in Supporting Information),[15] and characterized by NMR (Figures S1 and S2) and X-ray single crystal diffraction (Figure S3). The Gly-NTA single crystal belongs to the monoclinic crystal system (5.136 Å, 11.575 Å, 7.909 Å, 90°,

Received: August 18, 2023
Accepted: October 12, 2023

https://doi.org/10.1021/acsmacrolett.3c00491
ACS Macro Lett. 2023, 12, 1466−1471

Table 1. Copolymerization of Gly-NTA with Sar-NCA and zLL-NCA[a]

						DP[b]					
sample	NCA	$[Gly\text{-}NTA]_0$:$[NCA]_0$:$[initiator]_0$	temp. (°C)	time (h)	yield (%)	Gly	AA[c]	Gly[d] (%)	$M_{n,NMR}$[e] (kg/mol)	$M_{n,SEC}$[f] (kg/mol)	$Đ$[f]
1		50:0:1	30	42	37		0	100			
2	Sar	0:70:1	30	42	99	0	72	0	5.2	22.4	1.04
3	Sar	25:59:1	30	42	92	19	65	22.6	5.5	18.0	1.05
4	Sar	10:53:1	30	42	90	9	55	14.1	4.5	15.6	1.03
5	Sar	25:200:1	40	70	98	23	200	10.3	15.6	29.7	1.04
6	Sar	67:84:1	30	42	87	36	80	31.0	7.8	16.6	1.06
7	zLL	20:32:1	30	42	91	21	28	42.9	8.5	7.7	1.05
8	zLL	50:50:1	30	42	71	45	31	59.2	10.7	18.6	1.10
9	zLL	49:105:1	45	45	74	59	81	42.1	24.6	20.4	1.09

[a]Polymerization conditions: $[Gly]_0 + [NCA]_0 = 0.5$ mol/L, DMAc as solvent. Benzylamine and *n*-hexamine were used as the initiators for Sar-NCA and zLL-NCA, respectively. [b]Degree of polymerization, the average number of amino acid residues per polymer chain calculated by ^{1}H NMR. [c]Sar or zLL residue. [d]Molar fraction of Gly residues in copolymers calculated by ^{1}H NMR. [e]Determined by ^{1}H NMR. [f]Determined by SEC.

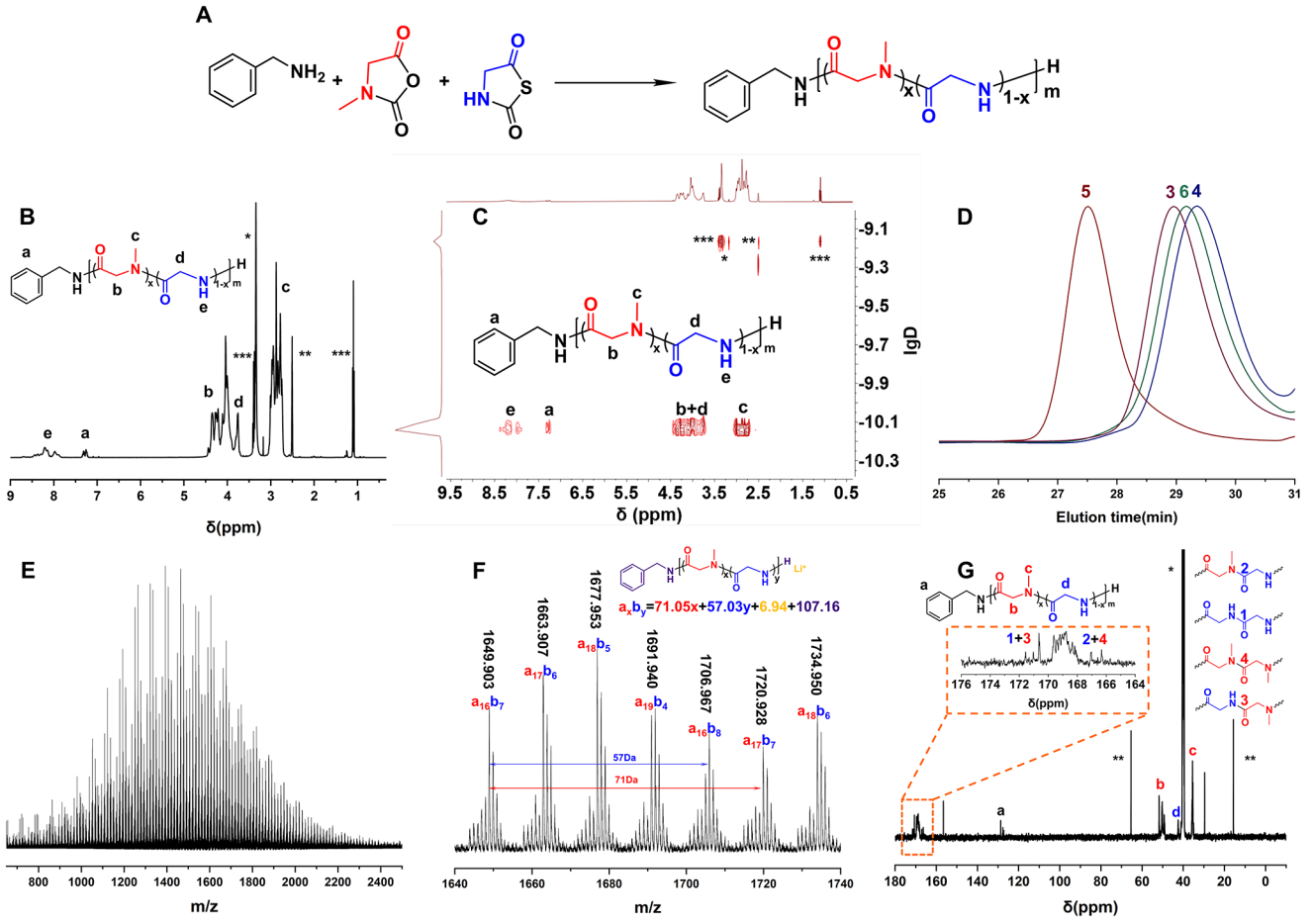

Figure 1. (A) Synthesis of PGS by the random copolymerization of Gly-NTA with Sar-NCA. (B) ^{1}H NMR spectrum of PGS, where *, **, and *** represent DMSO, water, and ether, respectively. (C) DOSY spectrum of PGS. (D) SEC traces of PGS copolymer samples in Table 1. (E, F) MALDI-ToF MS and a zoom-in view of PGS. (G) ^{13}C NMR spectrum of PGS, where * and ** represent DMSO and ether, respectively.

99.2°, 90°). Homopolymerization of Gly-NTA stops at limited conversion lower than 40% (sample **1** in Table 1) and white precipitates are observed within 5 min, which are insoluble in any solvent.

Copolymerizations of Gly-NTA with sarcosine NCA (Sar-NCA) (Figure S4) are well controlled at 30 °C in dimethylacetamide (DMAc; Figure 1A and samples **3**–**6** in Table 1) were performed without any precipitation or gelation. The copolymers of glycine with sarcosine poly(Gly-*r*-Sar) (PGS) exhibit symmetrically unimodal traces and narrow dispersities ($Đ$ < 1.1) in size-exclusion chromatography (SEC; Figure 1D). Both mass intervals of sarcosine (71 Da) and glycine residues (57 Da) are observed in the matrix-assisted laser desorption ionization time-of-flight mass spectrometry (MALDI-ToF MS) of PGS (Figure 1E,F). The absolute mass of each proportion with Li^+ cationization is consistent with the

https://doi.org/10.1021/acsmacrolett.3c00491
ACS Macro Lett. 2023, 12, 1466−1471

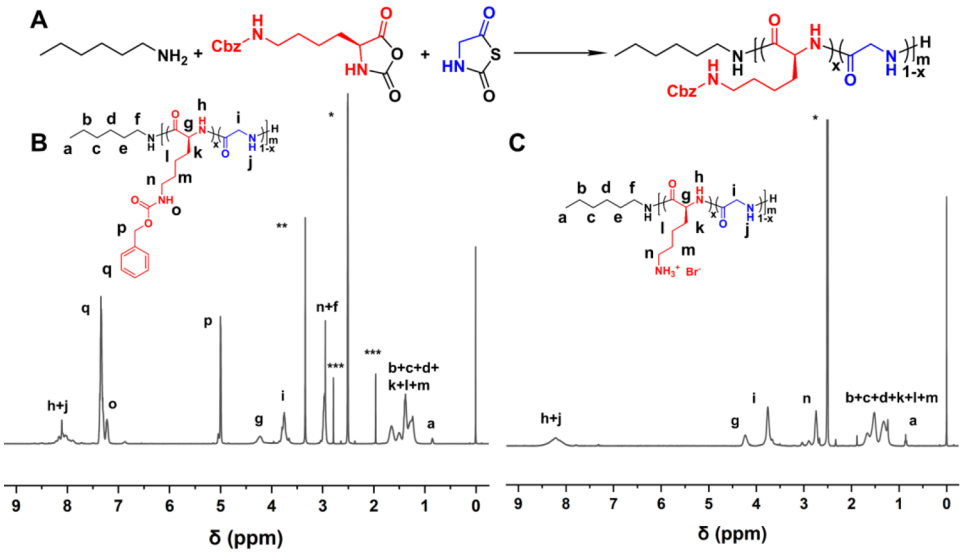

Figure 2. (A) Synthesis of PGZ by random copolymerization of Gly-NTA with zLL-NCA. (B) ^{1}H NMR spectrum of PGZ, where *, **, and *** represent DMSO, water, and DMAc, respectively. (C) ^{1}H NMR spectrum of PGK after deprotection.

corresponding composition of the random polymers (Figure 1E). The proton signals of both sarcosine and glycine residues are found at 2.65−3.05 ppm (methyl groups of sarcosine residues) and 3.65−4.45 ppm (α-H of both residues) in the ^{1}H NMR spectrum of PGS (Figure 1B). The content of glycine residues in the product increases with the initial feed ratio of [Gly-NTA]:[Sar-NCA], reaching a maximum of 31.0%, comparable to that in some GRPs.[2] The diffusion-ordered spectroscopy (DOSY) NMR spectrum suggests an identical diffusion coefficient (8.0×10^{-11} m^2/s, Figure 1C) of the protons in both the sarcosine and glycine residues. All the above prove the successful copolymerization of Gly-NTA with Sar-NCA.

Both the characterization of the copolymers and the kinetic study of the copolymerization reveal the comparable reactivities of Gly-NTA with Sar-NCA, which results in the random distribution of residues in PGS. The random topology of PGS is confirmed by ^{13}C NMR, heteronuclear single quantum coherence spectroscopy (HSQC), and heteronuclear multiple bond correlation (HMBC) analyses. The ^{13}C NMR and HSQC spectra determine the alkyl carbons of the polymer chain. The carbon signal of the methyl groups of sarcosine residues (C_c) locates at 35.1 ppm, while those at 42.0 ppm (C_d) and 48.3−51.4 ppm (C_b) are attributed to α-carbons (Figure 1G). Comparing the ^{13}C NMR spectra of PGS and polysarcosine in the acyl carbon region (Figure S5), we observe new signals between 170 and 172 ppm for PGS, representing two groups of acyl carbons neighboring secondary amines and primary amines. The ^{13}C NMR spectra of two model molecules also support the attribution (Figure S6). Moreover, these two carbonyl carbon signals are correlated to N−H and N−CH_3 in the HMBC spectrum (Figure S8). Accordingly, region I of the correlation signals around 8.0 ppm in Figure S8 is assigned to H_e-C_2, which represents Sar-Gly diads, while region II represents Gly-Gly diads. Similarly, the correlation signals of H_c-C_4 and H_c-C_3 indicate the presence of Sar-Sar and Gly-Sar diads.

The *in situ* Fourier transform infrared spectroscopy (FT-IR) technique is applied to explore the polymerization rates of Gly-NTA and Sar-NCA at 30 °C with a feed ratio of 25:50:1 ([Gly-NTA]$_0$/[Sar-NCA]$_0$/[BnNH$_2$]$_0$) in DMAc (Figure S9). The linear plots of time-dependent ln(M_0/M_t) support pseudo-first-order kinetics with two stages (Figure S10). The polymerization rate constants of Gly-NTA (1.8×10^{-3} min^{-1} in stage I and 4.9×10^{-3} min^{-1} in stage II) and Sar-NCA (2.0×10^{-3} min^{-1} in stage I and 5.5×10^{-3} min^{-1} in stage II) are very close to each other in both of the two stages, indicating the same consumption rates to produce random copolymers.

Lysine is a natural *C*-substituted amino acid, differing from sarcosine, with a *N*-methyl substitution. Random copolymerizations of Gly-NTA were performed with ε-Cbz-L-lysine NCA (zLL-NCA; Figure S11), which succeed and generate poly(Gly-*r*-zLL) (PGZ) copolymers (samples **7**−**9** in Table 1). The polymerization conditions are the same, except that *n*-hexamine is employed as the initiator instead of benzylamine to avoid the overlapping of the proton signals of phenyl groups. PGZ contains both Gly and zLL residues whose α-proton signals locate at 3.60−3.88 ppm and 4.15−4.30 ppm, respectively (Figure 2B), with identical coefficients in DOSY NMR (6.3×10^{-11} m^2/s, Figure S12). The MWs of PGZ are tunable between 8.5 and 24.6 kg/mol according to SEC and the dispersities of PGZ are narrow ($Đ < 1.1$). Both zLL-NCA and Gly-NTA exhibit pseudo-first-order kinetics (Figure S13). The linear plots of ln($[M]_0/[M]_t$) versus time reveal the livingness of polymerization and determine the comparable apparent polymerization rate constants of zLL-NCA (2.2×10^{-3} min^{-1}) and Gly-NTA (1.3×10^{-3} min^{-1}). Polypeptides consisting of glycine and L-lysine residues, poly(Gly-*r*-Lys) abbreviated as PGK, are obtained by the deprotection of the ε-carbobenzyloxy group under acidic conditions, evidenced by the disappearance of the signal at 7.4 ppm attributed to the benzyl group in ^{1}H NMR (Figure 2C).

We synthesized PGS and PGZ with controllable MWs (4.5−24.6 kg/mol) containing glycine residues from 10.3% to 59.2% and suppressed β-sheet folding during polymerization. The secondary structures are recoverable by workup procedure, solvent, temperature, pH, etc. FT-IR and circular dichroism (CD) are utilized to analyze the secondary structures of PGS, PGZ, and PGK. FT-IR spectrum of PGS (Figure S14A) and second derivative spectrum in amide I region (1600−1700

https://doi.org/10.1021/acsmacrolett.3c00491
ACS Macro Lett. 2023, 12, 1466−1471

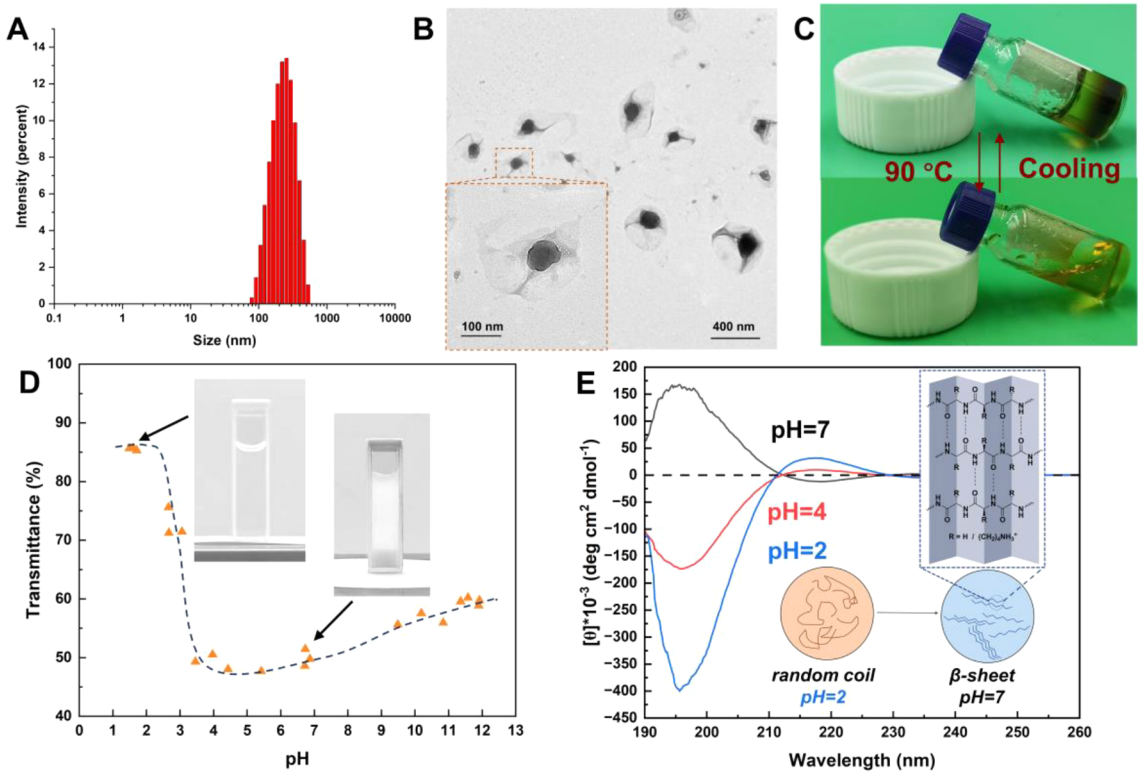

Figure 3. (A) DLS result of PGS micelles. (B) TEM image of PGS micelles. (C) Hydrogel generated from sample **6**. (D) pH-dependent transmittance changes of PGK titrated from basic to acidic condition. Inset: images of PGK in water at pH values of 2 and 7. (E) CD spectra of PGK at different pH values.

cm^{-1}, Figure S14B) reveal four peaks which are attributed to β-sheet (1642 cm^{-1}), α-helix (1652 cm^{-1}), β-turn (1669 cm^{-1}), and an unknown structure (1678 cm^{-1}).[20] CD spectra demonstrate β-sheet structures in PGZ (Figure S15A) and PGK (Figure S15B). The result indicates that the bulky side groups of zLL residues in glycine-rich PGZ backbones slightly disrupt the β-sheet folding.[21,22]

Glycine residues act as temperature-sensitive physical cross-linking points in PGS. PGS with 10% glycine residues (sample **5**) self-assembles into nanoparticles in water, showing an average diameter (D_h) of 240 nm in dynamic lighting scattering (DLS) measurements (Figure 3A). The transmission electron microscopy (TEM) image also supports their spherical morphologies with a diameter of ca. 100 nm (Figure 3B). Glycine residues aggregate through hydrogen bonding to construct the cores of the nanoparticles (black area in Figure 3B) and the shells are composed of sarcosine-rich regions. The sizes of the nanoparticles are tunable by temperature (Figure S16). The micelles disassemble under elevated temperatures (>40 °C) due to the destroyed hydrogen bonding. The glycine residues facilitate the formation of hydrogels through complex intermolecular interactions. Sample **6** containing 31% glycine residues forms a hydrogel with a water content up to 86.3% (Figure 3C), making it an attractive candidate for biomedical applications. The gel becomes flowable after 10 min heating at 90 °C, which is reversible back to gel by cooling at room temperature.

PGK keeps the β-sheet structure at a neutral pH when the pendant amine groups are protonated. PGK with 42% glycine residues exhibits a cloud point at a pH of 3.0 (Figure 3D). The CD spectra illustrate that PGK has a predominantly β-sheet character at neutral pH but transitions to random-coil character by decreasing the pH (Figure 3E). PGK maintains β-sheet structure when the pendant amine groups are mostly protonated at neutral pH while pK_a of the ε-NH_2 groups in poly-L-lysine is 9.3−9.5.[23] Differing from poly-L-lysine homopolymer, PGK demonstrates adjustable pH transition points of secondary structures in the acidic range, expanding the application of lysine-based responsive materials.[24−27]

In summary, we present a synthetic approach to glycine-rich PAAs with designable degree of polymerizations and narrow dispersities ($Đ$ < 1.1) by copolymerizations of Gly-NTA with Sar-NCA and zLL-NCA which have comparable reactivities to produce random copolymers. The first successful controlled polymerization of glycine is realized by inserting a second monomer in a random distribution to suppress β-sheet folding during polymerization, which is recoverable in proper conditions. PGS forms reversible temperature-sensitive hydrogel and nanoparticles in water when the content of glycine residues is 31% and 10%, respectively. PGK keeps the β-sheet structure at a neutral pH when the amine groups are protonated. The contribution fulfills the controllable synthesis of glycine-containing PAAs and opens up new possibilities for the precise design of glycine-based biomaterials.

■ ASSOCIATED CONTENT

Supporting Information

The Supporting Information is available free of charge at https://pubs.acs.org/doi/10.1021/acsmacrolett.3c00491.

Experimental section and the characterizations of monomers and random copolymers (^{1}H NMR, ^{13}C NMR, HSQC NMR, HMBC NMR, kinetic study, FT-IR spectra, circular dichroism spectra) (PDF)

https://doi.org/10.1021/acsmacrolett.3c00491
ACS Macro Lett. 2023, 12, 1466−1471

Gly-NTA single crystal (CIF)

Gly-NTA single crystal data (PDF)

AUTHOR INFORMATION

Corresponding Author

Jun Ling − *MOE Key Laboratory of Macromolecular Synthesis and Functionalization, Department of Polymer Science and Engineering, Zhejiang University, Hangzhou 310058, China;* orcid.org/0000-0002-0365-1381; Email: lingjun@zju.edu.cn

Authors

Jianping Wang − *MOE Key Laboratory of Macromolecular Synthesis and Functionalization, Department of Polymer Science and Engineering, Zhejiang University, Hangzhou 310058, China*

Peng Zhou − *MOE Key Laboratory of Macromolecular Synthesis and Functionalization, Department of Polymer Science and Engineering, Zhejiang University, Hangzhou 310058, China*

Ting Shen − *MOE Key Laboratory of Macromolecular Synthesis and Functionalization, Department of Polymer Science and Engineering, Zhejiang University, Hangzhou 310058, China*

Songyi Xu − *MOE Key Laboratory of Macromolecular Synthesis and Functionalization, Department of Polymer Science and Engineering, Zhejiang University, Hangzhou 310058, China*

Tianwen Bai − *MOE Key Laboratory of Macromolecular Synthesis and Functionalization, Department of Polymer Science and Engineering, Zhejiang University, Hangzhou 310058, China; College of Biological, Chemical Sciences and Engineering, Jiaxing University, Jiaxing 314001, China;* orcid.org/0000-0003-1033-9756

Complete contact information is available at: https://pubs.acs.org/10.1021/acsmacrolett.3c00491

Author Contributions

CRediT: **Jianping Wang** conceptualization, data curation, formal analysis, investigation, methodology, writing-original draft, writing-review & editing; **Peng Zhou** conceptualization, formal analysis, investigation, methodology, writing-original draft, writing-review & editing; **Ting Shen** formal analysis, investigation, methodology, writing-original draft, writing-review & editing; **Songyi Xu** formal analysis, investigation, writing-review & editing; **Tianwen Bai** data curation, formal analysis, funding acquisition, investigation; **Jun Ling** conceptualization, formal analysis, funding acquisition, investigation, methodology, project administration, resources, supervision, validation, writing-review & editing.

Notes

The authors declare no competing financial interest.

ACKNOWLEDGMENTS

Financial support by the National Natural Science Foundation of China (22271252, 22201105) and Starting Research Funds from Jiaxing University (CD70521025).

REFERENCES

(1) Gao, X.; Yin, C.; Liu, X.; Peng, J.; Chen, D.; He, D.; Shi, W.; Zhao, W.; Yang, J.; Peng, Y.-L. A Glycine-Rich Protein MoGrp1 Functions as a Novel Splicing Factor to Regulate Fungal Virulence and Growth in Magnaporthe Oryzae. *Phytopathol. Res.* **2019**, *1* (1), 2.

(2) Mousavi, A.; Hotta, Y. Glycine-Rich Proteins. *Appl. Biochem. Biotechnol.* **2005**, *120* (3), 169−174.

(3) Sachetto-Martins, G.; Franco, L. O.; de Oliveira, D. E. Plant Glycine-Rich Proteins: A Family or Just Proteins with a Common Motif? *Biochim. Biophys. Acta BBA - Gene Struct. Expr.* **2000**, *1492* (1), 1−14.

(4) Holland, G. P.; Creager, M. S.; Jenkins, J. E.; Lewis, R. V.; Yarger, J. L. Determining Secondary Structure in Spider Dragline Silk by Carbon−Carbon Correlation Solid-State NMR Spectroscopy. *J. Am. Chem. Soc.* **2008**, *130* (30), 9871−9877.

(5) Sponner, A.; Unger, E.; Grosse, F.; Weisshart, K. Differential Polymerization of the Two Main Protein Components of Dragline Silk during Fibre Spinning. *Nat. Mater.* **2005**, *4* (10), 772−775.

(6) Brannigan, J. A.; Wilkinson, A. J. Protein Engineering 20 Years On. *Nat. Rev. Mol. Cell Biol.* **2002**, *3* (12), 964−970.

(7) Mitchell, A. R. Bruce Merrifield and Solid-Phase Peptide Synthesis: A Historical Assessment. *Pept. Sci.* **2008**, *90* (3), 175−184.

(8) Merrifield, R. B. Solid Phase Peptide Synthesis. I. The Synthesis of a Tetrapeptide. *J. Am. Chem. Soc.* **1963**, *85* (14), 2149−2154.

(9) Tian, Z.-Y.; Zhang, Z.; Wang, S.; Lu, H. A Moisture-Tolerant Route to Unprotected α/β-Amino Acid N-Carboxyanhydrides and Facile Synthesis of Hyperbranched Polypeptides. *Nat. Commun.* **2021**, *12* (1), 5810.

(10) Rasines Mazo, A.; Allison-Logan, S.; Karimi, F.; Chan, N. J.-A.; Qiu, W.; Duan, W.; O'Brien-Simpson, N. M.; Qiao, G. G. Ring Opening Polymerization of α-Amino Acids: Advances in Synthesis, Architecture and Applications of Polypeptides and Their Hybrids. *Chem. Soc. Rev.* **2020**, *49* (14), 4737−4834.

(11) Lu, Y.; Gu, A.; Shen, T.; Sun, J.; Ling, J. Clickable, Oxidation-Responsive and Enzyme-Degradable Polypeptide: Synthesis, Characterization and Side Chain Modification. *Chin. J. Polym. Sci.* **2022**, *40* (11), 1360−1368.

(12) Lotz, B. Crystal Structure of Polyglycine I. *J. Mol. Biol.* **1974**, *87* (2), 169−180.

(13) Bykov, S.; Asher, S. Raman Studies of Solution Polyglycine Conformations. *J. Phys. Chem. B* **2010**, *114* (19), 6636−6641.

(14) Kricheldorf, H. R.; Schilling, G. ^{13}C NMR Sequence Analysis, 15. Copolymerization of Alanine-NCA with Other α-Amino Acid NCAs. *Makromol. Chem.* **1978**, *179* (5), 1175−1191.

(15) Zhou, P.; Shen, T.; Chen, W.; Sun, J.; Ling, J. Biodegradable Polysarcosine with Inserted Alanine Residues: Synthesis and Enzymolysis. *Biomacromolecules* **2022**, *23* (4), 1757−1764.

(16) Wang, S.; Chen, W.; Ling, J. PiPo: Random Copolymers of *C*-with *N*-Substituted Glycines. *Polym. Chem.* **2022**, *13* (3), 383−387.

(17) Fan, J.; Zou, J.; He, X.; Zhang, F.; Zhang, S.; Raymond, J. E.; Wooley, K. L. Tunable Mechano-Responsive Organogels by Ring-Opening Copolymerizations of N-Carboxyanhydrides. *Chem. Sci.* **2014**, *5* (1), 141−150.

(18) Tao, X.; Zheng, B.; Kricheldorf, H. R.; Ling, J. Are N-Substituted Glycine N-Thiocarboxyanhydride Monomers Really Hard to Polymerize? *J. Polym. Sci. Part Polym. Chem.* **2017**, *55* (3), 404−410.

(19) Zheng, B.; Xu, S.; Ni, X.; Ling, J. Understanding Acid-Promoted Polymerization of the N-Substituted Glycine N-Thiocarboxyanhydride in Polar Solvents. *Biomacromolecules* **2021**, *22* (4), 1579−1589.

(20) Dong, A.; Huang, P.; Caughey, W. S. Protein Secondary Structures in Water from Second-Derivative Amide I Infrared Spectra. *Biochemistry* **1990**, *29* (13), 3303−3308.

(21) Naik, S. S.; Ray, J. G.; Savin, D. A. Temperature- and PH-Responsive Self-Assembly of Poly(Propylene Oxide)-b-Poly(Lysine) Block Copolymers in Aqueous Solution. *Langmuir* **2011**, *27* (11), 7231−7240.

(22) Kelly, S. M.; Jess, T. J.; Price, N. C. How to Study Proteins by Circular Dichroism. *Biochim. Biophys. Acta (BBA)* **2005**, *1751* (2), 119−139.

(23) Ciucurel, E. C.; Sefton, M. V. A Poloxamine−Polylysine Acrylate Scaffold for Modular Tissue Engineering. *J. Biomater. Sci. Polym. Ed.* **2011**, *22* (18), 2515−2528.
(24) Chittchang, M.; Alur, H. H.; Mitra, A. K.; Johnston, T. P. Poly(L-lysine) as a Model Drug Macromolecule with Which to Investigate Secondary Structure and Membrane Transport, Part I: Physicochemical and Stability Studies. *J. Pharm. Pharmacol.* **2010**, *54* (3), 315−323.
(25) Yan, Y.; Wei, D.; Li, J.; Zheng, J.; Shi, G.; Luo, W.; Pan, Y.; Wang, J.; Zhang, L.; He, X.; Liu, D. A Poly(L-lysine)-Based Hydrophilic Star Block Co-Polymer as a Protein Nanocarrier with Facile Encapsulation and PH-Responsive Release. *Acta Biomater.* **2012**, *8* (6), 2113−2120.
(26) Kang, J.; Jeon, S. I.; Chung, I. J.; Ahn, C.-H. Functionalized PEG-Oligo(L-Lysine)-PCL Micelle System for the Delivery of Bioactive Agents Based on PH-Sensitive Degradation. *Funct. Compos. Struct.* **2020**, *2* (4), No. 045001.
(27) Zhou, P.; Li, Z.; Lu, Y.; Kong, J.; Ling, J. Telechelic Triblock Poly(α-Amino Acid)-Poly(Tetrahydrofuran)-Poly(α-Amino Acid) Copolymers: Chain-End Transformation, Polymerization and PH-Responsive Hydrolysis. *Chin. J. Chem.* **2021**, *39* (10), 2852−2856.

https://doi.org/10.1021/acsmacrolett.3c00491
ACS Macro Lett. 2023, 12, 1466−1471